10 (2022) 100136

Contents lists available at ScienceDirect

Biosensors and Bioelectronics: X

journal homepage: www.journals.elsevier.com/biosensors-and-bioelectronics-x

Quantitative detection of C-reactive protein in human saliva using an electrochemical lateral flow device

Loric Petruzzi [a,*], Thomas Maier [a], Peter Ertl [b], Rainer Hainberger [a]

[a] Molecular Diagnostics, AIT Austrian Institute of Technology GmbH, 1210, Vienna, Austria
[b] Faculty of Technical Chemistry, Institute of Applied Synthetic Chemistry, Vienna University of Technology, 1040, Vienna, Austria

ARTICLE INFO

Keywords:
Lateral flow device
LFD
Electrochemistry
Ascorbic acid
Alkaline phosphatase
Multiplexing
multiplex
Point-of-care
POC
Assay
Development
Optimization

ABSTRACT

Lateral flow devices (LFDs) allow for low-cost decentralized testing with a short time to result and are therefore an indispensable tool for point-of-care diagnostics. Here, we report on a novel LFD with electrochemical readout for the quantitative detection of C-reactive protein (CRP), a known biomarker for inflammation, in filtered human saliva and demonstrate the possibility of simultaneous multichannel measurements. The detection of CRP is enabled by a sandwich assay with target specific capture antibodies immobilized in a nitrocellulose membrane and target specific detection antibodies conjugated to an enzyme label. The subsequent enzymatic reaction leads to a product, which can be oxidized by an electrochemical sensor placed on top of the LFD strip and produce a concentration dependent and analyte specific electrical current. To optimize the system, single channel sensors were used to investigate different conjugate compositions and loads for their effect on assay performance. That way, limits of detection (LOD) of 3 and 25 ng/mL were achieved in buffer and filtered saliva, respectively. Then, a single sensor with four distinct channels was introduced for the testing of simultaneous multichannel measurements. There, the CRP dedicated channel showed a typical concentration dependency (with LODs of 13 and 55 ng/mL in buffer and filtered saliva, respectively), while the control channel expectedly produced elevated signals across all CRP concentrations. The signals corresponding to the other two channels (zeros) remained low with no indication of crosstalk, showing the ability to measure multiple locations on the LFD simultaneously and thus, paving the way for multiplexing.

1. Introduction

Point-of-care (POC) testing plays an increasingly important role in health care, both in resource-limited settings as well as in the aging societies of industrialized countries. Over the decades, the definition of POC evolved from "a medical test that is conducted at or near the site of patient care" (Kost, 2002) to a more unified concept, where the function (e.g. allowing a diagnosis and/or a change in patient management (Schito et al., 2012)) and the way a test device is used (e.g. by an untrained operator) are also taken into account. Based on this concept, the World Health Organization (WHO) developed the ASSURED (Kosack et al., 2017) criteria of ideal characteristics for POC tests. ASSURED stands for **a**ffordable, **s**ensitive, **s**pecific, **u**ser-friendly, **r**apid, **e**quipment-free and **d**elivered to those who need it. Although, the WHO specifically addressed resource-limited settings, to a large extent these criteria apply also for POC testing in other application scenarios.

Fast, simple, cheap and versatile are unique characteristics of lateral flow devices (LFDs), which have made them an indispensable tool for point-of-care testing (Guo et al., 2021; Mahmoudi et al., 2020; Soh et al., 2020; Posthuma-Trumpie et al., 2009). The working principle of LFDs relies on a capillary flow to transport a liquid sample through a porous nitrocellulose matrix. Capture molecules immobilized at predefined lines in the nitrocellulose matrix bind target molecules migrating with the sample, which leads to a local enrichment of the target molecules. The conjugation of the target molecules with a signal generator allows qualitative or quantitative transduction of the biochemical reaction to a measurable signal. LFDs are developed to be sensitive and specific enough to support or indicate a diagnosis with statistical relevance, while being optimized for user-friendliness and for the number of operations required by the user. Plus, LFDs are small devices that can be supplied to and operated in a highly decentralized setup without major logistical or environmental burden. Moreover, LFDs can be produced in large number which greatly reduces the fabrication costs.

The most common type of LFD relies on gold or latex nanoparticles

* Corresponding author.
E-mail address: loric.petruzzi@ait.ac.at (L. Petruzzi).

https://doi.org/10.1016/j.biosx.2022.100136
Received 13 January 2022; Received in revised form 18 March 2022; Accepted 23 March 2022
Available online 27 March 2022

used as signal indicators. The agglomeration of these nanoparticles in the capture lines creates a colored band, which is visually assessed (O'Farrell et al., 2009) by the user, usually resulting in a simple yes/no result. A quantification of this colorimetric result is possible using optical LFD readers, which convert the degree of coloring to an analyte concentration (Urusov et al., 2019; Cheng et al., 2017; Parolo et al., 2013a, 2013b). Further transduction methods for LFDs include fluorescent (Borse and Srivastava, 2019; Chen et al., 2018; Cai et al., 2018; Cheeveewattanagul et al., 2017; Wu et al., 2018), chemiluminescence (Zangheri et al., 2015), Raman spectrocopy (Kim et al., 2021; Fu et al., 2016) and electrochemical approaches (Akanda and Ju, 2018; Ruiz--Vega et al., 2017; Zou et al., 2012; Wang et al., 2011; Sinawang et al., 2016; Du et al., 2012; Yoon et al., 2003). Also the use of thermal cameras (Jia et al., 2019) or magnetic field fluctuations (Taton et al., 2009) has been investigated. Table 1 provides an overview on these different signal transduction methods uses in lateral flow devices.

Although most lateral flow devices detect single target analytes, there are also examples of multiplexed LFDs allowing the detection of several target analytes at the same time. Examples include commercially available drug of abuse screening LFDs using colorimetry (D2rug Abuse Mult, 2021) or quantitative assays using magnetic particle quantification (Guteneva et al., 2019). LFDs can be developed for almost any bodily fluid relevant for medical diagnostics (Koczula and Gallotta, 2016), such as whole blood, serum, plasma, saliva, nasal secretions, urine and sweat among others. Saliva in particular, is a matrix that gained importance in medical diagnostics over the past decade (Malamud, 2011; Pink et al., 2009), and even more during the ongoing pandemic of SARS-CoV-2 (Wang et al., 2020, 2021; Suleman et al., 2021).

Saliva offers several great POC advantages: it is readily available in comparison to whole blood or serum (Kaufman and Lamster, 2002; Sri Santosh et al., 2020), contains many relevant biomarkers and, more importantly, its sampling procedure is highly convenient because of its noninvasiveness, speed and it being stress free for the patient (Aro et al., 2017; Khan et al., 2017), making it an easy and cost efficient way to collect probes. On the other hand, saliva is also associated with a few major challenges. In addition to saliva complex composition and unusual physical properties, biomarkers are typically found at a much lower concentration than in blood, which necessitates highly sensitive measurement methods. Moreover, the amounts of analytes found in saliva are not always correlated to their counterpart in blood (Bel'skaya et al., 2020), which can complicate accurate diagnostics. Finally, drinking or eating before taking a salivary test or even a lack of oral hygiene are all contaminations that can affect the reliability and performance of the diagnostic device. Nevertheless, saliva stays a relevant biofluid as it has been used to develop a wide variety of diagnostic tests to detect proteins (C-reactive protein (Dillon et al., 2010), ferritin (Gawaly and Alghazaly, 2020)), hormones (cortisol (PETERS et al., 1982), aldosterone (Hubl et al., 1983)), antibodies (Ada et al., 2020), viruses (COVID-19 (Santana et al., 2020; Fabiani et al., 2021), HIV (Tamashiro and Constantine, 1994), hepatitis A (Parry et al., 1989)), microbes (*H.pylori* (Li et al., 1996), *Shigella* (Schultz et al., 2020)) or even drugs (Drobitch and Svensson, 1992).

A major limitation of conventional LFDs is associated with the lack of sensitivity, which is particularly problematic with saliva samples and their inherent lower analyte concentrations. Owing to their electrical output signal and high sensitivity, electroanalytical sensing techniques are suited to overcome these limitations. These detection methods can easily be interfaced with readily available electronic read-out units such as smartphones or computers, which paves the way not only for miniaturization and system integration but also and especially for quantitative POC diagnostics. Moreover, electrochemical methods do not rely on external factors such as varying lighting conditions or on the nonlinear behavior of imaging sensors. Previous work underlines the pertinence of the combination between saliva and electrochemistry, for example with the successful detection of cortisol (Kämäräinen et al., 2018), tetrahydrocannabinol (Stevenson et al., 2019) or lithium ions (Suherman et al., 2019) using different electrodes and approaches.

This paper aims at combining the specificity of immunoassays with the sensing power of electrochemical reactions into an LFD for the measurement of biomarkers in saliva. More specifically, we report the implementation of an electrochemical assay on an LFD platform for the quantitative detection of C-reactive protein (CRP) in saliva. CRP is a biomolecule used as biomarker for inflammation (Pepys and Hirschfield, 2003). It can be found in blood (10^3–10^4 ng/mL) (Okamura et al., 1990) as well as in saliva, however in much lower amounts (10^2 to 10^3 times less) (Floriano et al., 2009; Ouellet-Morin et al., 2011). In our approach, CRP quantification is achieved by capturing the protein with a specific antibody and relaying an electrical signal using the enzymatic activity of streptavidin-alkaline phosphatase (SALP), which is conjugated to a biotinylated detection antibody specific for CRP, with respect to the substrate ascorbic acid monophosphate (AAP). The latter reaction produces ascorbic acid, which is an electroactive molecule that can be readily oxidized into dehydroascorbic acid (dAA) by the action of a sufficiently large electrical potential. Ultimately, the oxidation turnover is dependent on the amount of CRP captured and induce a concentration dependent electrical signal. The goal of this study is to achieve concentration dependent and relevant quantitative signals for CRP in saliva. Additionally, a multi-electrode sensor will be used to assess the multiplex capabilities of the developed electrochemical lateral flow setup. The choice to use screen-printed sensors is motivated by their inherent high flexibility in their design and printing substrate as well as for their low price per unit achievable when considering high volume manufacturing.

2. Materials and methods

2.1. Materials and LFD fabrication

Streptavidin-coupled Alkaline phosphatase (SALP) was purchased from Roche (art. 11093266910) at a stock concentration of 750 U/mL. Monoclonal mouse anti-human CRP antibody (art. MAB17071), biotinylated mouse monoclonal anti-human CRP antibody (dAB) (art. BAM17072) and goat anti-mouse IgG antibody (art. AF007) were purchased from R&D Systems. Human CRP (art. C1617), L-ascorbic acid (art. 33034), L-ascorbic acid 2-phosphate sesquimagnesium salt hydrate

Table 1
Summary of possible signal transduction methods for quantitative LFDs with respective target and linear range.

TRANSDUCTION METHOD	TARGET	LINEAR RANGE	REFERENCES
Colorimetric	Human IgG	0–500 ng/mL	Parolo et al. (2013b)
Fluorescence	*E. coli*	50-10^4 cfu/mL	(Cheeveewattanagul et al., 2017; Wu et al., 2018)
Chemiluminescence	Cortisol	0.3–60 ng/mL	Zangheri et al. (2015)
Raman spectroscopy	HIV-1 DNA	0.008–64 ng/mL	Fu et al. (2016)
Electrochemical (voltammetry)	NS1 protein	1–25 ng/mL	Sinawang et al. (2016)
Electrochemical (voltammetry)	Troponin I	0.1–1 ng/mL	Du et al. (2012)
Electrochemical (electrochemiluminescence)	*Legionella* antigen	2–10^4 ng/mL	Yoon et al. (2003)
Thermal	*E. coli*	2*10^4-2*10^7 cfu/mL	Jia et al. (2019)
Magnetic	Interferon gamma	12–1000 pg/mL	Taton et al. (2009)

(AAP) (art. A8960), Sodium Chloride (art. 71376) and Trizma hydrochloride (art. 93363) were obtained from Sigma-Aldrich. The latter salts were used for the buffer preparation, which followed the recommendations of the supplier for SALP as well as supported by the literature (James et al., 2002) and is a 100 mM Tris-HCl and 150 mM NaCl mixture adjusted at pH 7.5 with NaOH 4 M for enzyme dilution and to 9.0 to run the LFDs. Bovine serum albumin fraction V (BSA) was acquired from Merck (art. 112018). Lateral flow strips were prepared by laminating the nitrocellulose membranes (Merck Millipore, Hi-Flow Plus HFC180UB 40 mm × 300 mm) onto backing cards obtained from Kenosha (KN–V1080.217, 80 mm × 300 mm), which are used for physical support for the nitrocellulose membrane and the connected pads. The conjugate pad is placed on the backing card with a 1 mm overlap with the membrane. The sample pad is applied by keeping a similar overlap with the conjugate pad. LFD are then cut from the backing card in approximately 3.3 mm wide stripes using a manual guillotine (Dahle 562). Antibody lines were deposited at a concentration of 1 mg/mL on the nitrocellulose using a line dispenser (ClaremontBio, Model: ALFRD) coupled to a syringe pump to achieve a dispensing rate of 1 μL/cm. The capture line for CRP is printed using the monoclonal mouse anti-human CRP antibody, while the control line is printed using the goat anti-mouse IgG antibody from R&D Systems. Once printed, the membranes were dried at room temperature for 60 min and stored at 4 °C in a closed plastic bag together with desiccant until further use. The glass fiber conjugate pad (Merck Millipore, GFCP103000, 10 mm × 300 mm) and the cellulose fiber sample pad (Merck Millipore, CFSP173000 17 mm × 300 mm) were prepared as follow: the enzyme-labeled conjugate was prepared by mixing amounts of dAB with SALP using Tris buffer at pH 9.0 as diluent. After mixing the two components, the solutions were incubated for 60 min at room temperature to achieve complete streptavidin-biotin binding. Conjugate pads were then fully soaked with this solution and dried at room temperature overnight. Sample pads were fully soaked with in a solution containing 100 mM AAP with 1% (w/v) BSA in Tris buffer at pH 9.0 and dried at room temperature overnight. Following the lamination of the conjugate and sample pad, the membranes were cut into strips with a width of approximately 3.3 mm and stored in a container with a bag of desiccant at 4 °C until further use. For the preparation of filtered saliva samples, full saliva was filtered using a syringe filter (Pall Acrodisc 25 mm Syringe Filter, GxF/0.45 μm GHP-Membrane, PN AP-4559) and spiked with CRP. A visual inspection of the conjugate binding to the test and control line is achieved by using a color developer (Thermo Fisher, art. 34042), in which the strips are soaked after running them with the sample and drying them for at least 1 h.

2.2. Electrochemical LFD principle

The LFD described in this paper used C-reactive protein (CRP) as analyte in a sandwich type immunoassay involving one capture and one control line, which were printed on a nitrocellulose surface using anti-CRP and anti-IgG antibodies, respectively. When a sample is applied on the sample pad (Fig. 1A), the liquid migrates toward the opposite end of the strip by capillary action. The sample pad contains the electrochemically inactive substrate (AAP), which is dissolved in the sample liquid. Next, the liquid enters the conjugate pad containing the detection antibody bound to an enzymatic label. As the sample passes the conjugate pad, the conjugate binds to the CRP present in the sample. Further downstream, the liquid reaches the CRP-specific capture line, where the CRP-conjugate assemblies bind to the CRP-specific capture antibodies. Conjugates passing the CRP-specific capture test line are enriched in the

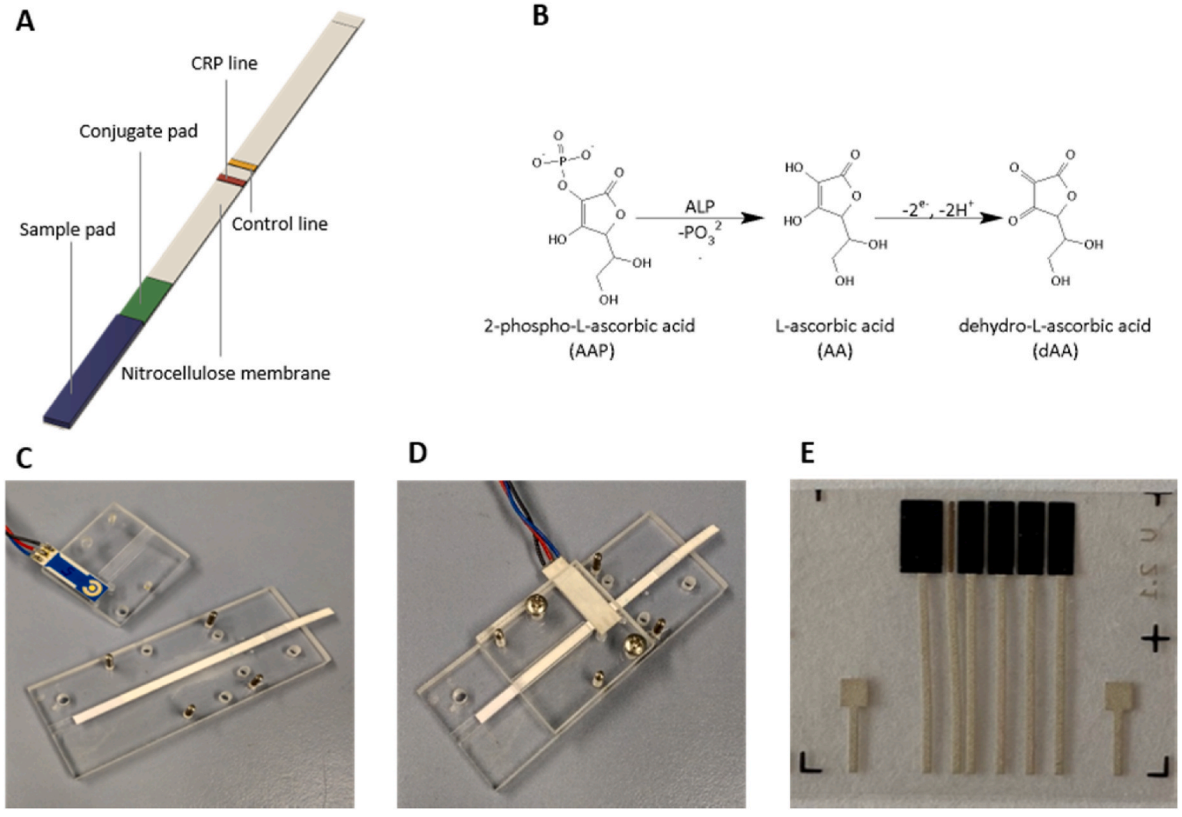

Fig. 1. **A** Schematic illustration of the electrochemical lateral flow device. **B** Chemical equation describing the enzymatic dephosphorylation of 2-phospho-L-ascorbic acid (AAP) into L-ascorbic acid (AA) and its subsequent oxidation into dehydro-L-ascorbic acid (dAA), which is the reaction used to generate an electrical signal at the electrode in the electrochemical LFD. **C** and **D** are pictures of the single electrode electrochemical measurement setup with the LFD strip before and after mounting the electrochemical sensor, respectively. **E** Screen-printed sensor used for multiple simultaneous measurements experiments. From left to right: counter electrode, reference electrode and working electrodes 1–4.

control line situated after the test line. The enzyme, now locally enriched on the lines of the respective capture antibodies, converts AAP into AA, thus locally augmenting the generation of electroactive material. An electrochemical sensor is positioned with its working electrode right above the test line. That way an analyte specific current can be measured by applying an oxidizing voltage to the working electrode turning AA into dehydroascorbic acid (dAA) (Fig. 1B).

2.3. Electrochemical measurements procedures

2.3.1. Linear sweep voltammetry

Linear sweep voltammetry was carried out using a single channel sensor (BVT, Type AC1.W1.R1) connected to an Autolab PGSTAT-101 potentiostat (Metrohm AG, Switzerland) using the following parameters: scan range from −0.3 to 0.5 V and scan rate 0.05 V/s. For these measurements, the sensor was positioned face up and 200 μL of sample was deposited at its surface in a way to form a drop that covered all sensor electrodes. The measurement was started using the software and, when finished, the sample was removed with an absorbent paper and the sensor cleaned with deionized water for further use.

2.3.2. Chronoamperometric measurements

Two distinct types of electrochemical sensors were used to obtain an electrochemical readout from the LFDs. For single-channel measurements on the CRP-selective capture line, a commercially available screen-printed sensor with a 2 mm diameter round shaped gold working electrode, a ring-shaped gold counter electrode, and a ring-shaped Ag/AgCl reference electrode (BVT, Type AC1.W1.R1) was used (see Fig. 1C). Multi-channel measurements were performed with a screen-printed sensor with four-line shaped carbon working electrodes with 2 mm pitch, one carbon counter electrode and one AgCl reference electrode on PRT foil, fabricated by SCIO Holding GmbH, Austria (Fig. 1E). For a better handling, the sensors were attached to dedicated holders, which allowed a precise positioning of with respect to the LFD by means of guiding pins on the base plate and holes in the sensor holder. After placing the LFD on the measuring platform (Fig. 1C), the sensor holder was brought in place above the LFD and fixed with screws (Fig. 1D). The chronoamperometric measurement procedure with a working electrode potential of 0.4 V was started together with the application of 100 μL of sample liquid on the sample pad. After the completion of the measurement, the sensor holder was removed, the LFD discarded, and the sensor briefly washed with deionized water and dried in a nitrogen stream for the next measurement. With this procedure, the same sensor is used for each measurement of a concentration dependence. The repeatability of the sensors was tested by measuring the chronoamperometric response to a solution of 100 mM ascorbic acid in Tris buffer pH 9.0 applied on the sensor surface. The coefficients of variation for measuring this target and washing in between measurements is 5 and 8% (n = 7), for the BVT and the multi-channel screen-printed sensor, respectively. Single-channel measurements were performed using a Autolab PGSTAT-101 potentiostat (Metrohm AG, Switzerland), while a 4-channel polypotentiostat EmStat3 4WE (Palmsens BV, the Netherlands) was used for the simultaneous multiple measurements.

2.4. Data analysis

The chronoamperometric currents measured at a defined time after sample application are the concentration dependent signals measures that were considered for further data analysis. The signals were analyzed using a sigmoidal four-parameters fit (Holstein et al., 2015). For each concerned data set, the sigmoidal four-parameters function was fitted to evaluate the data. In the formula below, a, b, c and d are the fitting parameters, C the concentration of analyte, and S the measured signal.

$$S = \frac{a-d}{1+\left(\frac{\log(C)}{c}\right)^{b}} + d$$

The limit of detection (LOD) is calculated by taking the average of a zero-calibrator set of measurements plus three time its standard deviation and solving the fitted model for C. All calculations were made using OriginPro 2021b (v9.8.5.204), the models were fitted using the Levenberg Marquardt algorithm. The parameters obtained after fitting are displayed in table T1 of the supplementary material.

3. Results & discussion

3.1. Detection principle and time trace

In a first step, we investigated the electrochemical properties of the assay components to determine a suitable potential window for the detection of the product of the enzymatic reaction. The linear sweep measurements plotted in Fig. 2A show that a minimum potential of at least 0.1–0.2 V is required to effectively oxidize AA, which is also in line with what is found in literature (Sapper et al., 1982; Deakin et al., 1986; Matsui et al., 2015). Compared to Tris buffer, containing no electrochemically active components, the signal in saliva remains on the same low level for potentials below 0.4 V, but shows a significant rise for higher voltages. To achieve effective oxidation of AA while keeping the electrochemical response from saliva at a minimum, we therefore chose 0.4 V as potential for the chronoamperometric measurements. Furthermore, no signal rise is observed for 100 mM AAP in buffer, indicating that AAP is not electrochemically active by itself. The conversion of AAP to AA is demonstrated by mixing AAP with 7.5 U of ALP for 10 min prior to the measurement, after which a strong electrochemical response from AA is observed. In other words, electrical saliva signals (grey line) do not interfere with the measurement of the result of the enzymatic reaction (green line). This leads to the possibility to measure a reaction specific electrical signal during the assay, despite the presence of saliva.

Following the electrochemical system suitability testing, the concept of the immunoassay is tested. To this end, a set of measurements was performed using LFDs with a single printed test line of CRP-specific antibodies and a single channel electrode. In total, six different CRP concentrations were used for the evaluation. Fig. 2B shows the corresponding time traces of the chronoamperometric measurements, where t = 0 denotes the application of the sample liquid on the LFD. The temporal evolution of the curves can be interpreted in the following way: the first event is a sharp rise in current at 100 s related to the liquid reaching the electrode. The migrating liquid is already loaded with electroactive AA because of the enzymatic reaction that started earlier in the conjugate pad. As the liquid continues its way through the strip, the current continues to rise until about 400 s, when the liquid reaches the end of the membrane and causes the flow to halt. Without further AA supply from the conjugate pad, the current first drops and then gradually stabilizes to a slow and steady linear decrease after approximately 600 s, after which the current reflects the amount of conjugate immobilized below the electrode and thus the CRP concentration in the sample.

3.2. Optimization of conjugate composition

As the conjugate formed by the enzyme (SALP) and the CRP detection antibody (dAB) is an essential part of the assay, the impact of various combinations of SALP and dAB on the assay performance were investigated. For this purpose, chronoamperometric measurements over 900 s were performed for LFDs carrying different amounts and compositions of the conjugate. Fig. 3 shows the electrochemical signal of different sets of LFDs and indicates where a concentration dependent signal has been observed. The first three experiments were made with increasing total amount of material in the conjugate pad, while keeping the ratio between SALP and dAB constant. With higher loading, the dynamic range and the resolution increased reaching the range of interest between 1 and 10 ng/mL for the third iteration. To assure that the assay was not hampered by an excess of unbound SALP or dAB, two

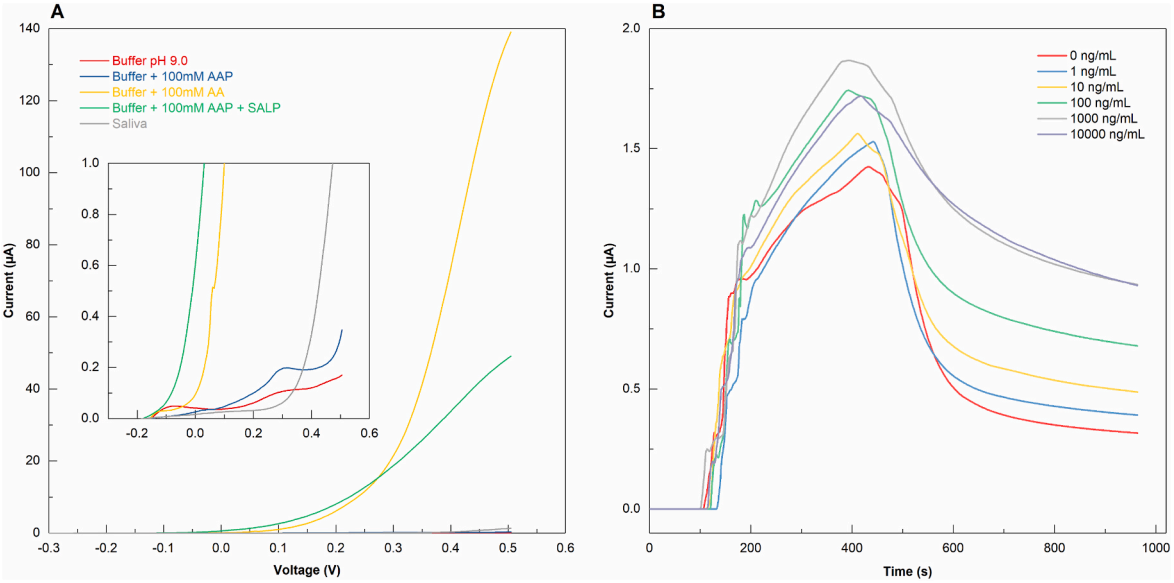

Fig. 2. **A** Linear sweep voltammograms for Tris buffer pH 9.0, ascorbic acid monophosphate (AAP), ascorbic acid (AA) and AAP mixed with streptavidin alkaline phosphatase (SALP). **B** Single channel chronoamperometric measurements in LFDs with different CRP concentrations in buffer, the applied voltage is 0.4 V.

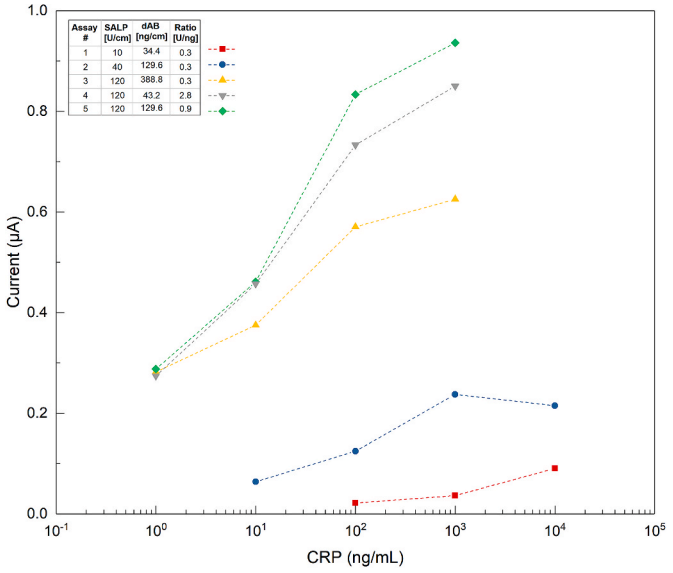

Fig. 3. CRP concentration dependence in LFDs with varying conjugate composition and conjugate load. Data points represent the current after 900 s from the sample application. SALP stands for Streptavidin Alkaline Phosphatase, dAB for detection antibody (biotinylated).

additional assays with constant amount of SALP but different amounts of dAB were performed. This further increased the dynamic range of the assay. Optimum conditions were reached for assay number five with an SALP to dAB ratio of 0.9 U/ng. These assay parameters were used for all subsequent experiments. Additionally, the stability of the dried form of the SALP was investigated (Fig. S1 in the supplementary data) over eight months while stored at 4 °C. There was no statistical change (two sample *t*-test with pooled variance, $p(x \leq T) = 0.255$) in the enzymatic activity for AAP dephosphorylation over that time. Meaning that the SALP can be prepared and stored for a long period of time without losing in activity and potentially hurting the assay performance.

3.3. Single channel measurements

Saliva is a complex medium for immunoassays. It contains a number of different proteins such as mucins and enzymes, which not only increase viscosity (Noiphung et al., 2018) but also can interfere with the binding of antibodies (Fulton et al., 1989) and influence the diffusion of molecules in it. Depending on the analyte, other types of influences from the oral cavity (e.g. microbial flora, cavities) (Miočević et al., 2017) may also affect the assay performance. In order to minimize the effects of the sample matrix on the assay performance, more or less complex sample pretreatment procedures involving dilution or centrifugation of saliva are common (Mitchell and Lowe, 2009), and various collection procedures (Kidd et al., 2009; Mohamed et al., 2012) and collection devices have been developed. To stay in line with the goal to keep the use of the assay simple, we restricted the saliva preparation to a filtering step as described in section 3.1. Fig. 4 shows a comparison of the calibration curves achieved in buffer and filtered saliva. A clear CRP dependence is observed in both cases. The most striking difference between the two curves is the reduction of the measured electrical current in saliva by roughly a factor of 2.5. We attribute this reduction to the higher viscosity of the saliva samples, which hinders the diffusion of the product to the electrode surface. Furthermore, the LOD increases from 3 ng/mL in buffer to 25 ng/mL in saliva.

3.4. Evaluating multiplexing capabilities

The simultaneous measurement capabilities of the system were investigated using an electrochemical sensor with four working electrodes (Fig. 1E). The first of these working electrodes were aligned with the CRP-specific capture antibodies on the nitrocellulose, while the third working electrode was aligned with the anti-mouse antibody line (control). Working electrodes 2 and 4 covered untreated areas on the nitrocellulose strip. Fig. 5A and B plot the chronoamperometric measurement results for different CRP concentrations in Tris buffer and filtered saliva, respectively. The CRP-specific signals show a similar behavior as already shown in the previous single-channel measurements. Comparing the signals in buffer and filtered saliva, the linear domain is reduced by a factor 10 on both the upper and lower end, and the estimated LOD increases from 13.5 in buffer to 55 ng/mL. The signal decrease for high CRP concentrations ($>10^4$ ng/mL) is attributed to the Hook effect (Schiettecatte et al., 2012). Therefore, the corresponding

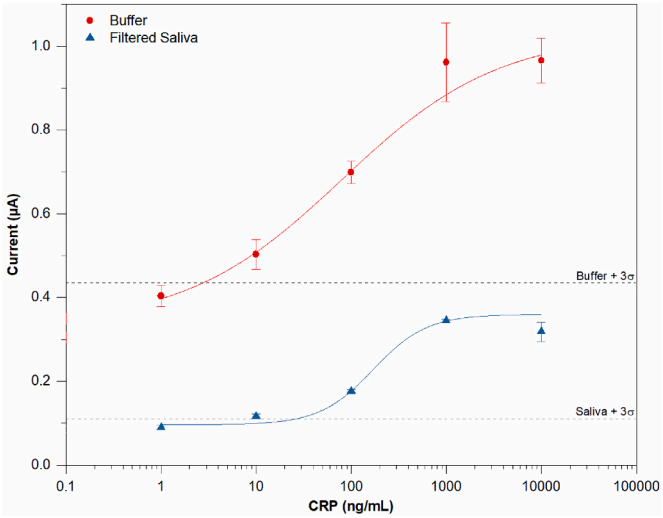

Fig. 4. Single channel experiments with spiked amounts of C-reactive protein (CRP) in Tris buffer pH 9.0 and filtered saliva. Each data point is taken from a chronoamperometric measurement at t = 900 s and represents the average of n = 3 with according to errors bars. The dashed lines represent the average signal of a set of blank measurements (non-spiked saliva) of n = 5 plus three time its standard deviation. The parameters obtained after fitting of the datasets following section 3.4 and used for calculations are provided in table T1 of the supplementary material.

data points were not considered for the mathematical fitting.

Regarding the control line, the electrochemical signal is elevated for all CRP concentrations confirming the occurrence of binding events at this location. At higher concentrations, the signal is reduced as an immediate consequence of the high binding occurrence at the test line (see Supplementary Fig. S2). To achieve a higher degree of saturation across the CRP range, higher amounts of conjugate (SALP and dAB) would have to be used. However, more SALP would also increase the baseline signal (see Fig. 3), which would worsen the performance of the assay. Instead, we use the properties of this signal as a dynamic control: the elevated signal at all concentrations allows to confirm the proper migration and binding of the conjugate at the control line, similarly to a classical control. However, in this case the difference of signal between both extremes also enables to verify the interaction of the conjugate with CRP as its signal decreases with an increased CRP content.

Finally, WEs 2 and 4 signals, where there are no capture molecules, remain low across all CRP concentrations, which indicates that the individual working electrodes act independently of each other, and that there is no crosstalk between neighboring regions on the strips. This opens the possibility to detect additional target molecules by implementing other target specific capture and detection antibodies. Additionally, this also means that no sign of nonspecific interactions between the capture molecules for CRP and saliva was found.

The discrepancy between the LODs measured with single (Fig. 4) and multi-channel (Fig. 5) sensors can be explained with the difference of the working electrode area between both experiments, which use different sensors. We have shown that an increase in electrode area (supplementary material, Fig. S3) is associated with a greater standard variation for a set of measurements. Therefore, the change in LOD observed between both sensors is expected because of the variation introduced due to a larger electrode.

Moreover, the assay has potential for further improvement. The work by *Young Kyoung* Oh et al. (2014) provides with a good example. Their quantitative lateral flow includes an innovative approach involving a three-lines system, merging a direct and a competitive assay. The advantage is that low CRP concentrations are measured with the competitive assay, while the direct assay takes care of the higher values. This approach ensures a consistent signal over a large dynamic range. Given the ability to measure more than one line at the time with our LFD, this concept could potentially be adapted. There also exist other options for improvement such as the use of a robust same preparation procedure for saliva or the use of different types of nitrocellulose membranes, sample and conjugate pads, sensor geometries, conjugate additives, or the application of diverse blocking agents.

4. Conclusion

A quantitative electrochemical LFD was developed and subsequently investigated regarding its potential for CRP quantification in saliva. In doing so, the voltametric and chronoamperometric experiments allowed to establish a proper potential for the detection of the enzymatic product, to verify the suitability of the electrochemical system and to subsequently demonstrate a CRP concentration dependent signal. Then, the conjugate composition was investigated by looking at the effect of different combinations of SALP and dAB, which lead to improvements in dynamic range and sensitivity by a factor 10^3. Single channel electrode measurements with Tris buffer and saliva highlighted the importance of a salivary sample pre-treatment procedure for obtaining a reliable assay. The added complexity of saliva (complex, physical properties, lower concentrations) lead to lower electrical current and slightly worse performances, however still in a relevant range. Subsequently, the system was tested with a sensor comprising four working electrodes allowing the measurement at up to four different locations on the nitrocellulose membrane. The sensor was able to simultaneously measure concentration dependent signals on two different working electrodes using Tris buffer and saliva. It was demonstrated that the LFD system can return concentration dependent signals in saliva with the possibility to measure several targets simultaneously. Furthermore, this study showed that this technology has the potential to be adapted into a multiplexing (up to four targets) electrochemical lateral flow device, which could be further enhanced into a fully portative device for POC applications.

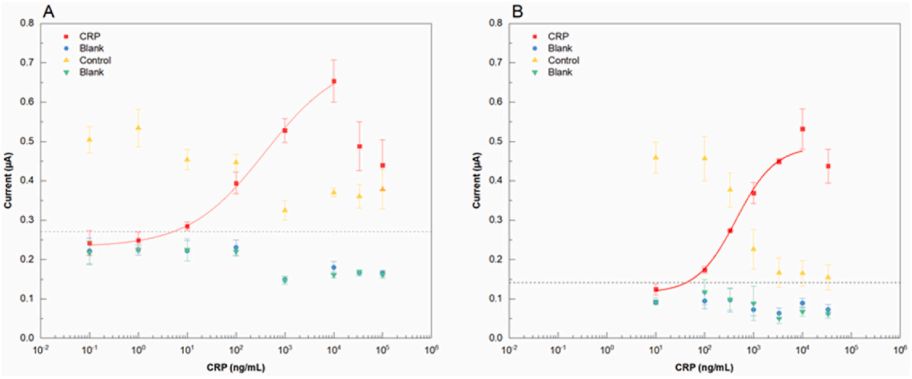

Fig. 5. Endpoint current at t = 900 s for different concentrations of CRP on a screen-printed sensor with four working electrodes positioned above capture antibodies for specific molecules: WE1: CRP, WE2: no capture molecules, WE3: control, WE4: no capture molecules. Each CRP concentration represents an average with n = 3. The dashed bars represent the average signal of a set of blank measurements (n = 5) plus three time its standard deviation. The parameters obtained after fitting of the datasets following section 3.4 and used for calculations are provided in table T1 of the supplementary material. **A** Data obtained when measuring CRP in Tris buffer pH 9.0. **B** Data obtained when measuring CRP in filtered human saliva.

CRediT authorship contribution statement

Loric Petruzzi: Conceptualization, Methodology, Validation, Formal analysis, Investigation, Writing – original draft, Writing – review & editing, Visualization. **Thomas Maier:** Conceptualization, Investigation, Methodology, Validation, Data curation, Writing – review & editing, Visualization, Supervision. **Peter Ertl:** Writing – review & editing, Visualization. **Rainer Hainberger:** Conceptualization, Writing – review & editing, Supervision, Project administration, Funding acquisition.

Declaration of competing interest

The authors declare that they have no known competing financial interests or personal relationships that could have appeared to influence the work reported in this paper.

Acknowledgements

This research has received funding from the European Union's Horizon 2020 research and innovation program under grant agreement No 761167 (IMPETUS).

Appendix A. Supplementary data

Supplementary data to this article can be found online at https://doi.org/10.1016/j.biosx.2022.100136.

References

Ada, Aita, Basso, Daniela, Cattelan, Anna Maria, et al., 2020. SARS-CoV-2 identification and IgA antibodies in saliva: one sample two tests approach for diagnosis. Clin. Chim. Acta 510, 717–722. https://doi.org/10.1016/j.cca.2020.09.018.

Akanda, M.R., Ju, H., 2018. Ferritin-triggered redox cycling for highly sensitive electrochemical immunosensing of protein. Anal. Chem. 90, 8028–8034. https://doi.org/10.1021/acs.analchem.8b00933.

Aro, K., Wei, F., Wong, D.T., et al., 2017. Saliva liquid biopsy for point-of-care applications. Front. Public Health 5, 77. https://doi.org/10.3389/fpubh.2017.00077.

Bel'skaya, Lyudmila V., Sarf, Elena A., Kosenok, Victor K., 2020. Age and gender characteristics of the biochemical composition of saliva: correlations with the composition of blood plasma. J Oral Biol Craniofac Res 10, 59–65. https://doi.org/10.1016/j.jobcr.2020.02.004.

Borse, V., Srivastava, R., 2019. Fluorescence lateral flow immunoassay based point-of-care nanodiagnostics for orthopedic implant-associated infection. Sensor. Actuator. B Chem. 280, 24–33. https://doi.org/10.1016/j.snb.2018.10.034.

Cai, Y., Kang, K., Liu, Y., et al., 2018. Development of a lateral flow immunoassay of C-reactive protein detection based on red fluorescent nanoparticles. Anal. Biochem. 556, 129–135. https://doi.org/10.1016/j.ab.2018.06.017.

Cheeveewattanagul, N., Morales-Narváez, E., Hassan, A.-R.H.A., et al., 2017. Straightforward immunosensing platform based on graphene oxide-decorated nanopaper: a highly sensitive and fast biosensing approach. Adv. Funct. Mater. 27, 1702741. https://doi.org/10.1002/adfm.201702741.

Chen, J., Huang, Z., Meng, H., et al., 2018. A facile fluorescence lateral flow biosensor for glutathione detection based on quantum dots-MnO2 nanocomposites. Sensor. Actuator. B Chem. 260, 770–777. https://doi.org/10.1016/j.snb.2018.01.101.

Cheng, N., Song, Y., Zeinhom, M.M.A., et al., 2017. Nanozyme-mediated dual immunoassay integrated with smartphone for use in simultaneous detection of pathogens. ACS Appl. Mater. Interfaces 9, 40671–40680. https://doi.org/10.1021/acsami.7b12734.

MED2WORLD drug abuse multiple test – urine. https://new.med2world.com/index.php/product-details/drug-abuse-multiple-test-urine/. (Accessed April 2021).

Deakin, M.R., Kovach, P.M., Stutts, K.J., et al., 1986. Heterogeneous mechanisms of the oxidation of catechols and ascorbic acid at carbon electrodes. Anal. Chem. 58, 1474–1480. https://doi.org/10.1021/ac00298a046.

Dillon, M.C., Opris, D.C., Kopanczyk, R., et al., 2010. Detection of homocysteine and C-reactive protein in the saliva of healthy adults: comparison with blood levels. Biomark. Insights 5, 57–61. https://doi.org/10.4137/bmi.s5305.

Drobitch, R.K., Svensson, C.K., 1992. Therapeutic drug monitoring in saliva. Clin. Pharmacokinet. 23, 365–379. https://doi.org/10.2165/00003088-199223050-00003.

Du, D., Wang, J., Wang, L., et al., 2012. Integrated lateral flow test strip with electrochemical sensor for quantification of phosphorylated cholinesterase: biomarker of exposure to organophosphorus agents. Anal. Chem. 84, 1380–1385. https://doi.org/10.1021/ac202391w.

Fabiani, Laura, Saroglia, Marco, Galatà, Giuseppe, et al., 2021. Magnetic beads combined with carbon black-based screen-printed electrodes for COVID-19: a reliable and miniaturized electrochemical immunosensor for SARS-CoV-2 detection in saliva. Biosens. Bioelectron. 171, 112686. https://doi.org/10.1016/j.bios.2020.112686.

Floriano, P.N., Christodoulides, N., Miller, C.S., et al., 2009. Use of saliva-based nanobiochip tests for acute myocardial infarction at the point of care: a feasibility study. Clin. Chem. 55, 1530–1538. https://doi.org/10.1373/clinchem.2008.117713.

Fu, X., Cheng, Z., Yu, J., et al., 2016. A SERS-based lateral flow assay biosensor for highly sensitive detection of HIV-1 DNA. Biosens. Bioelectron. 78, 530–537. https://doi.org/10.1016/j.bios.2015.11.099.

Fulton, A., Chan, S., Coleman, G., 1989. Effect of salivary proteins on binding curves of three radioimmunoassay kits: amerlex-M progesterone, Amerlex cortisol, and Biodata testosterone. Clin. Chem. 35, 641–644. https://doi.org/10.1093/clinchem/35.4.641.

Gawaly, A., Alghazaly, G., 2020. Serum & salivary ferritin levels in iron deficiency anemia is there is a difference? Hematology. Transf. Cell Ther. 42, 56. https://doi.org/10.1016/j.htct.2020.09.101.

Guo, J., Chen, S., Guo, J., et al., 2021. Nanomaterial labels in lateral flow immunoassays for point-of-care-testing. J. Mater. Sci. Technol. 60, 90–104. https://doi.org/10.1016/j.jmst.2020.06.003.

Guteneva, N.V., Znoyko, S.L., Orlov, A.V., et al., 2019. Rapid lateral flow assays based on the quantification of magnetic nanoparticle labels for multiplexed immunodetection of small molecules: application to the determination of drugs of abuse. Mikrochim. Acta 186, 621. https://doi.org/10.1007/s00604-019-3726-9.

Holstein, C.A., Griffin, M., Hong, J., et al., 2015. Statistical method for determining and comparing limits of detection of bioassays. Anal. Chem. 87, 9795–9801. https://doi.org/10.1021/acs.analchem.5b02082.

Hubl, W., Taubert, H., Freymann, E., et al., 1983. A simple solid phase enzyme immunoassay for aldosterone in plasma and saliva. Exp. Clin. Endocrinol. 82, 188–193. https://doi.org/10.1055/s-0029-1210275.

James, Hethey, Lai, Jacqueline, Loutet, Slade, et al., 2002. Effects of tricine, Glycine and tris buffers on alkaline phosphatase. Activity 2, 33–38.

Jia, M., Liu, J., Zhang, J., et al., 2019. An immunofiltration strip method based on the photothermal effect of gold nanoparticles for the detection of Escherichia coli O157: H7. Analyst 144, 573–578. https://doi.org/10.1039/C8AN01004H.

Kämäräinen, S., Mäki, M., Tolonen, T., et al., 2018. Disposable electrochemical immunosensor for cortisol determination in human saliva. Talanta 188, 50–57. https://doi.org/10.1016/j.talanta.2018.05.039.

Kaufman, Eliaz, Lamster, Ira B., 2002. The diagnostic applications of saliva— a review. Crit. Rev. Oral Biol. Med. 13, 197–212. https://doi.org/10.1177/154411130201300209.

Khan, R.S., Khurshid, Z., Yahya Ibrahim Asiri, F., 2017. Advancing point-of-care (PoC) testing using human saliva as liquid biopsy. Diagnostics 7. https://doi.org/10.3390/diagnostics7030039.

Kidd, S., Midgley, P., Lone, N., et al., 2009. A re-investigation of saliva collection procedures that highlights the risk of potential positive interference in cortisol immunoassay. Steroids 74, 666–668. https://doi.org/10.1016/j.steroids.2009.02.009.

Kim, K., Kashefi-Kheyrabadi, L., Joung, Y., et al., 2021. Recent advances in sensitive surface-enhanced Raman scattering-based lateral flow assay platforms for point-of-care diagnostics of infectious diseases. Sensor. Actuator. B Chem. 329, 129214. https://doi.org/10.1016/j.snb.2020.129214.

Koczula, K.M., Gallotta, A., 2016. Lateral flow assays. Essays Biochem. 60, 111–120. https://doi.org/10.1042/EBC20150012.

Kosack, C.S., Page, A.-L., Klatser, P.R., 2017. A guide to aid the selection of diagnostic tests. Bull. World Health Organ. 95, 639–645. https://doi.org/10.2471/BLT.16.187468.

Kost, G.J., 2002. Principles & Practice of Point-of-care Testing. Lippincott Williams & Wilkins.

Li, C., Ha, T., Ferguson, D.A., et al., 1996. A newly developed PCR assay ofH. pylori in gastric biopsy, saliva, and feces. Dig. Dis. Sci. 41, 2142–2149. https://doi.org/10.1007/BF02071393.

Mahmoudi, T., La Guardia, M de, Baradaran, B., 2020. Lateral flow assays towards point-of-care cancer detection: a review of current progress and future trends. Trac. Trends Anal. Chem. 125, 115842. https://doi.org/10.1016/j.trac.2020.115842.

Malamud, D., 2011. Saliva as a diagnostic fluid. Dent. Clin. 55, 159–178. https://doi.org/10.1016/j.cden.2010.08.004.

Matsui, T., Kitagawa, Y., Okumura, M., et al., 2015. Accurate standard hydrogen electrode potential and applications to the redox potentials of vitamin C and NAD/NADH. J. Phys. Chem. 119, 369–376. https://doi.org/10.1021/jp508308y.

Miočević, O., Cole, C.R., Laughlin, M.J., et al., 2017. Quantitative lateral flow assays for salivary biomarker assessment: a review. Front. Public Health 5, 133. https://doi.org/10.3389/fpubh.2017.00133.

Mitchell, J.S., Lowe, T.E., 2009. Matrix effects on an antigen immobilized format for competitive enzyme immunoassay of salivary testosterone. J. Immunol. Methods 349, 61–66. https://doi.org/10.1016/j.jim.2009.07.012.

Mohamed, R., Campbell, J.-L., Cooper-White, J., et al., 2012. The impact of saliva collection and processing methods on CRP, IgE, and Myoglobin immunoassays. Clin. Transl. Med. 1, e19. https://doi.org/10.1186/2001-1326-1-19.

Noiphung, J., Nguyen, M.P., Punyadeera, C., et al., 2018. Development of paper-based analytical devices for minimizing the viscosity effect in human saliva. Theranostics 8, 3797–3807. https://doi.org/10.7150/thno.24941.

Oh, Y.K., Joung, H.-A., Han, H.S., et al., 2014. A three-line lateral flow assay strip for the measurement of C-reactive protein covering a broad physiological concentration range in human sera. Biosens. Bioelectron. 61, 285–289. https://doi.org/10.1016/j.bios.2014.04.032.

Okamura, J.M., Miyagi, J.M., Terada, K., et al., 1990. Potential clinical applications of c-reactive protein. J. Clin. Lab. Anal. 4, 231–235. https://doi.org/10.1002/jcla.1860040316.

Ouellet-Morin, I., Danese, A., Williams, B., et al., 2011. Validation of a high-sensitivity assay for C-reactive protein in human saliva. Brain Behav. Immun. 25, 640–646. https://doi.org/10.1016/j.bbi.2010.12.020.

O'Farrell, B., 2009. Evolution in lateral flow–based immunoassay systems. In: Wong, R., Tse, H. (Eds.), Lateral Flow Immunoassay. Humana Press, Totowa, NJ, pp. 1–33.

Parolo, C., Medina-Sánchez, M., La Escosura-Muñiz, A de, et al., 2013a. Simple paper architecture modifications lead to enhanced sensitivity in nanoparticle based lateral flow immunoassays. Lab Chip 13, 386–390. https://doi.org/10.1039/c2lc41144j.

Parolo, C., La Escosura-Muñiz, A de, Merkoçi, A., 2013b. Enhanced lateral flow immunoassay using gold nanoparticles loaded with enzymes. Biosens. Bioelectron. 40, 412–416. https://doi.org/10.1016/j.bios.2012.06.049.

Parry, J.V., Perry, K.R., Mortimer, P.P., et al., 1989. Diagnosis of hepatitis a and b by testing saliva. J. Med. Virol. 28, 255–260. https://doi.org/10.1002/jmv.1890280410.

Pepys, M.B., Hirschfield, G.M., 2003. C-reactive protein: a critical update. J. Clin. Invest. 111, 1805–1812. https://doi.org/10.1172/JCI200318921.

Peters, J.R., Walker, R.F., Dr, F., et al., 1982. Salivary cortisol assays for assessing pituitary-adrenal reserve. Clin. Endocrinol. 17, 583–592. https://doi.org/10.1111/j.1365-2265.1982.tb01631.x.

Pink, R., Simek, J., Vondrakova, J., et al., 2009. Saliva as a diagnostic medium. Biomed. Pap. Med. Fac. Univ. Palacky Olomouc Czech Repub 153, 103–110. https://doi.org/10.5507/bp.2009.017.

Posthuma-Trumpie, G.A., Korf, J., Amerongen, A., 2009. Lateral flow (immuno)assay: its strengths, weaknesses, opportunities and threats. A literature survey. Anal. Bioanal. Chem. 393, 569–582. https://doi.org/10.1007/s00216-008-2287-2.

Ruiz-Vega, G., Kitsara, M., Pellitero, M.A., et al., 2017. Electrochemical lateral flow devices: towards rapid immunomagnetic assays. Chemelectrochem 4, 880–889. https://doi.org/10.1002/celc.201600902.

Sapper, Helmut, , Sa-Ouk Institut für Biophysik der Justus-Liebig-Universität Gießen, Leihgestemer Weg 217, D-6300 Gießen, Paul, Hans-Helmut, et al., 1982. The reversibility of the vitamin C redox system: electrochemical reasons and biological aspects. Z. Naturforsch. C Biosci. 37, 942–946. https://doi.org/10.1515/znc-1982-1015.

Schiettecatte, Johan, Anckaert, Ellen, Smitz, Johan, 2012. Interferences in immunoassays: 3. In: Chiu, Norman H.L., Christopoulos, Theodore K. (Eds.), Advances in Immunoassay Technology. IntechOpen, Rijeka.

Schito, M., Peter, T.F., Cavanaugh, S., et al., 2012. Opportunities and challenges for cost-efficient implementation of new point-of-care diagnostics for HIV and tuberculosis. J. Infect. Dis. 205 (Suppl. 2), S169–S180. https://doi.org/10.1093/infdis/jis044.

Schultz, J., Uddin, Z., Singh, G., et al., 2020. Glutamate sensing in biofluids: recent advances and research challenges of electrochemical sensors. Analyst 145, 321–347. https://doi.org/10.1039/C9AN01609K.

Sinawang, P.D., Rai, V., Ionescu, R.E., et al., 2016. Electrochemical lateral flow immunosensor for detection and quantification of dengue NS1 protein. Biosens. Bioelectron. 77, 400–408. https://doi.org/10.1016/j.bios.2015.09.048.

Soh, J.H., Chan, H.-M., Ying, J.Y., 2020. Strategies for developing sensitive and specific nanoparticle-based lateral flow assays as point-of-care diagnostic device. Nano Today 30, 100831. https://doi.org/10.1016/j.nantod.2019.100831.

Sri Santosh, T., Parmar, R., Anand, H., et al., 2020. A review of salivary diagnostics and its potential implication in detection of covid-19. Cureus 12, e7708. https://doi.org/10.7759/cureus.7708.

Stevenson, H., Bacon, A., Joseph, K.M., et al., 2019. A rapid response electrochemical biosensor for detecting thc in saliva. Sci. Rep. 9, 12701. https://doi.org/10.1038/s41598-019-49185-y.

Suherman, A.L., Rasche, B., Godlewska, B., et al., 2019. Electrochemical detection and quantification of lithium ions in authentic human saliva using LiMn2O4-modified electrodes. ACS Sens. 4, 2497–2506. https://doi.org/10.1021/acssensors.9b01176.

Suleman, S., Shukla, S.K., Malhotra, N., et al., 2021. Point of care detection of COVID-19: advancement in biosensing and diagnostic methods. Chem. Eng. J. 414, 128759. https://doi.org/10.1016/j.cej.2021.128759.

Tamashiro, H., Constantine, N.T., 1994. Serological diagnosis of HIV infection using oral fluid samples. Bull. World Health Organ. 72, 135–143.

Taton, K., Johnson, D., Guire, P., et al., 2009. Lateral flow immunoassay using magnetoresistive sensors. J. Magn. Magn Mater. 321, 1679–1682. https://doi.org/10.1016/j.jmmm.2009.02.113.

Urusov, A.E., Zherdev, A.V., Dzantiev, B.B., 2019. Towards lateral flow quantitative assays: detection approaches. Biosensors 9. https://doi.org/10.3390/bios9030089.

Vaz, S.N., de Santana, D.S., Netto, E.M., Pedroso, C., Wang, W.-K., Santos, F.D.A., Brites, C., 2020. Saliva is a reliable, non-invasive specimen for SARS-CoV-2 detection. Braz. J. Infect. Dis. 24, 422–427. https://doi.org/10.1016/j.bjid.2020.08.001.

Wang, L., Lu, D., Wang, J., et al., 2011. A novel immunochromatographic electrochemical biosensor for highly sensitive and selective detection of trichloropyridinol, a biomarker of exposure to chlorpyrifos. Biosens. Bioelectron. 26, 2835–2840. https://doi.org/10.1016/j.bios.2010.11.008.

Wang, C., Horby, P.W., Hayden, F.G., et al., 2020. A novel coronavirus outbreak of global health concern. Lancet 395, 470–473. https://doi.org/10.1016/S0140-6736(20)30185-9.

Wang, C., Liu, M., Wang, Z., et al., 2021. Point-of-care diagnostics for infectious diseases: from methods to devices. Nano Today 37, 101092. https://doi.org/10.1016/j.nantod.2021.101092.

Wu, R., Zhou, S., Chen, T., et al., 2018. Quantitative and rapid detection of C-reactive protein using quantum dot-based lateral flow test strip. Anal. Chim. Acta 1008, 1–7. https://doi.org/10.1016/j.aca.2017.12.031.

Yoon, C.-H., Cho, J.-H., Oh, H.-I., et al., 2003. Development of a membrane strip immunosensor utilizing ruthenium as an electro-chemiluminescent signal generator. Biosens. Bioelectron. 19, 289–296. https://doi.org/10.1016/S0956-5663(03)00207-0.

Zangheri, M., Cevenini, L., Anfossi, L., et al., 2015. A simple and compact smartphone accessory for quantitative chemiluminescence-based lateral flow immunoassay for salivary cortisol detection. Biosens. Bioelectron. 64, 63–68. https://doi.org/10.1016/j.bios.2014.08.048.

Zou, Z.-X., Wang, J., Wang, H., et al., 2012. An integrated electrochemical device based on immunochromatographic test strip and enzyme labels for sensitive detection of disease-related biomarkers. Talanta 94, 58–64. https://doi.org/10.1016/j.talanta.2012.02.046.